

# Light-dependence of Formate (C1) and Acetate (C2) Transport and Oxidation in Poplar Trees

Kolby J. Jardine (✉ [kjjardine@lbl.gov](mailto:kjjardine@lbl.gov))

Lawrence Berkeley National Laboratory

Joseph Lei

Lawrence Berkeley National Laboratory

Suman Som

Lawrence Berkeley National Laboratory

Daisy Souza

National Institute for Amazon Research

Chaevien S. Clendinen

Pacific Northwest National Laboratory

Hardeep Mehta

Pacific Northwest National Laboratory

Pubudu Handakumbura

Pacific Northwest National Laboratory

Markus Bill

Lawrence Berkeley National Laboratory

Robert P. Young

Pacific Northwest National Laboratory

Eoin Brodie

Lawrence Berkeley National Laboratory

---

## Method Article

**Keywords:** Acetate fermentation, carbon assimilation, formate, trees, xylem injection, day respiration, glyoxylate cycle

**Posted Date:** March 22nd, 2022

**DOI:** <https://doi.org/10.21203/rs.3.rs-1463360/v1>

**License:**   This work is licensed under a Creative Commons Attribution 4.0 International License.

[Read Full License](#)

---

# Abstract

## Background

Although apparent light inhibition of leaf day respiration is a widespread reported phenomenon, the mechanisms involved, including utilization of alternate respiratory pathways and substrates and light inhibition of TCA cycle enzymes are under active investigation. Recently, acetate fermentation was highlighted as a key drought survival strategy mediated through protein acetylation and jasmonate signaling. Here, we evaluate the light-dependence of acetate transport and assimilation in *Populus trichocarpa* trees using a new dynamic xylem solution injection (DXSI) method for continuous studies of C<sub>1</sub> and C<sub>2</sub> organic acid transport and light-dependent metabolism.

## Results

Over 7 days, 1.0 L of [<sup>13</sup>C]formate and [<sup>13</sup>C<sub>2</sub>]acetate solutions were delivered to the stem base of 2-year old potted poplar trees, while continuous diurnal observations were made in the canopy of CO<sub>2</sub>, H<sub>2</sub>O, and isoprene gas exchange together with δ<sup>13</sup>CO<sub>2</sub>. Stem base injection of 10 mM [<sup>13</sup>C<sub>2</sub>]acetate induced an overall pattern of canopy branch headspace <sup>13</sup>CO<sub>2</sub> enrichment (δ<sup>13</sup>CO<sub>2</sub> +27‰) with a diurnal structure in δ<sup>13</sup>CO<sub>2</sub> reaching a mid-day minimum following by a maximum shortly after darkening where δ<sup>13</sup>CO<sub>2</sub> values rapidly increased up to +12‰. In contrast, 50 mM injections of [<sup>13</sup>C]formate were required to reach similar δ<sup>13</sup>CO<sub>2</sub> enrichment levels in the canopy with δ<sup>13</sup>CO<sub>2</sub> following diurnal patterns of transpiration. Illuminated leaves of detached poplar branches pretreated with 10 mM [<sup>13</sup>C<sub>2</sub>]acetate showed lower δ<sup>13</sup>CO<sub>2</sub> (+20‰) compared to leaves treated with 10 mM [<sup>13</sup>C]formate (+320‰), the opposite pattern observed at the whole plant scale.

Following dark/light cycles at the leaf-scale, rapid, strong, and reversible enhancements in headspace δ<sup>13</sup>CO<sub>2</sub> by up to +60‰ were observed in [<sup>13</sup>C<sub>2</sub>]acetate treated leaves which showed enhanced dihydrojasmonic acid and TCA cycle intermediate concentrations.

## Conclusions

The results are consistent with acetate in the transpiration stream as an effective activator of the jasmonate signaling pathway and respiratory substrate. The shorter lifetime of formate relative to acetate in the transpiration stream suggests rapid formate oxidation to CO<sub>2</sub> during transport to the canopy. In contrast, acetate is efficiently transported to the canopy where an increased allocation towards mitochondrial dark respiration occurs at night. The results highlight the potential for an effective integration of acetate into glyoxylate and TCA cycles and the light-inhibition of citrate synthase as an important regulatory mechanism in controlling the diurnal allocation of acetate between anabolic and catabolic processes.

# Background

Aerobic respiration is a biochemical process requiring oxygen that occurs in living plant cells and provides usable chemical energy, reducing power, and carbon skeletons needed in numerous physiological processes including growth and development, reproduction, tissue maintenance/defense during stress, and senescence [1]. In higher plants, mitochondrial aerobic respiratory activity is also known to be critical for optimizing photosynthetic metabolism, especially during periods of abiotic stress which can lead to over-reduction of mitochondria and/or chloroplasts and excessive production of reactive oxygen species [2]. Fueled by the central  $C_2$  metabolite acetyl-CoA, the tricarboxylic acid cycle (TCA) in mitochondria produces respiratory  $CO_2$  that can be re-assimilated by photosynthesis, or emitted from leaves via stomata to the atmosphere. While acetyl-CoA production from pyruvate decarboxylation catalyzed by mitochondrial pyruvate dehydrogenase (PDH) is the typical pathway for aerobic respiration of non-structural carbohydrates via glycolysis [3], alternative respiratory pathways active during abiotic stress are also under investigation [4]. Two alternative respiratory pathways receiving increasing attention are the oxidative  $C_1$  pathway and acetate fermentation ( $C_2$ ). The  $C_1$  pathway, whose quantitative importance in plant carbon cycling is largely unknown, starts with the release of methanol from primary cell-walls [5] and ends with the generation of  $CO_2$  in both mitochondria and chloroplasts during formate oxidation [6]. Recently, plant tissue concentrations of acetate were shown to dramatically increase due to the activation of acetate fermentation during drought stress [7, 8]. Acetate accumulation stimulates the jasmonate (JA) signaling pathway mediated by histone H4 acetylation to confer drought tolerance [7]. Upregulation of acetate fermentation is considered an evolutionarily conserved drought survival strategy, with the amount of acetate produced directly correlating to survival. While the signaling roles of acetate have been discussed in terms of protein acetylation, its active form as acetyl-CoA is the major respiratory substrate entering the TCA cycle [9] and used in the synthesis of a numerous primary and secondary metabolites including fatty acids, terpenoids, hydrocarbons, polyketides and flavonoids [10]. In contrast to acetate/acetic acid which may travel long distances in plants via the transpiration stream, acetyl-CoA is impermeable to membranes and is generally required to be synthesized within each organelle [10]. Thus, activation of acetate to acetyl-CoA may be a key mechanism of supplying alternative sources of acetyl-CoA to organelles with high catabolic (e.g. mitochondria) and anabolic (e.g. peroxisome, chloroplast) demands. Therefore, acetyl-CoA, the biologically active form of acetate, links anabolic and catabolic processes and coordinates metabolism with cellular signaling by mediating protein acetylation and serving as a key substrate for biosynthetic and respiratory reactions [10].

Leaf respiration in  $C_3$  plants during the day has been widely discussed as light-inhibited relative to the dark [11, 12], although this change in respiratory flux is uncertain because of difficulties in separating simultaneous  $CO_2$  sources (e.g. respiration and photorespiration) and  $CO_2$  sinks (e.g. photosynthesis) [13]. The biochemical causes of the apparent light suppression of leaf respiration are under active investigation and include a decrease in the photochemical efficiency of photosystem II with irradiance, an increasing proportion of photorespiration with irradiance as well as refixation of internal  $CO_2$  sources (respiration, photorespiration,  $C_1$  pathway, etc.) by photosynthesis, and an actual decrease of

mitochondrial respiratory rates due to light inhibition of key enzymes including mitochondrial pyruvate dehydrogenase (PDH) and citrate synthase [14, 15]. In addition, coordinated interactions of respiratory substrates with other biochemical pathways during the day may also be involved [15, 16]. For example, biosynthetic pathways active during the day such as light-dependent *de novo* fatty acid biosynthesis in chloroplasts, which utilize identical substrates as mitochondrial respiration (e.g. acetate/acetyl-CoA) [17]. Leaf day respiration involves many biochemical and enzymatic reactions that interact with light [15]. Through its impact on enzyme activity, light is known to exert a strong control over respiratory substrate allocation to biosynthetic versus catabolic metabolism. For example, plant cells have both a mitochondrial and plastidal form of pyruvate dehydrogenase (PDH) that catalyzes the oxidative decarboxylation of pyruvate to acetyl-CoA. The mitochondrial form is highly active in the dark compared with the light and generates acetyl-CoA for use in the TCA cycle during aerobic respiration. In contrast, the plastidal form of PDH provides acetyl-CoA for *de novo* fatty acid biosynthesis with a higher activity in the light compared with the dark [3]. Consistent with the view of the differential light controls over the mitochondrial and chloroplast forms of PDH, a recent study concluded that light inhibition of the mitochondrial form of PDH can largely explain the apparent light suppression of leaf day respiration relative to dark respiration in sunflower [18].

In addition to the PDH reaction which generates acetyl-CoA from pyruvate, light inhibition of citrate synthase (CS), which condenses acetyl-CoA with oxaloacetate as the first step of the TCA cycle in mitochondria, has also been demonstrated [19]. However, the quantitative importance of CS light inhibition in suppressing TCA cycle decarboxylations in the light remains unclear. In order to bypass the PDH reaction and evaluate potential light inhibition of the CS reaction, in this study, we supplied acetate via the transpiration stream to detached and intact poplar trees. We hypothesized that acetate in the transpiration stream of trees can be used as a respiratory substrate in leaves via activation to acetyl-CoA and that acetate allocation to the TCA cycle in the light (day respiration) is suppressed by CS light inhibition. To evaluate the possibility of CS light inhibition, we bypassed the normal production of acetyl-CoA via the mitochondrial PDH reaction by supplying external [ $^{13}\text{C}_2$ ]acetate via the transpiration stream and quantified diurnal respiratory emission of  $^{13}\text{CO}_2$ .

Photosynthesis with atmospheric  $^{13}\text{CO}_2$  is regularly used to trace plant and ecosystem fates of recently assimilated carbon, including as substrates for stem and soil respiration [20]. However, novel approaches are being investigated including the direct injection of isotopically labeled substances into the xylem of trees including  $\text{D}_2\text{O}$  [21],  $\text{H}_2^{18}\text{O}$  [22], and  $\text{H}^{13}\text{CO}_3^-$  [23]. For example, xylem injections of  $\text{D}_2\text{O}$  have been used to characterize whole-tree water transport and storage properties [21]. Direct xylem injections of  $\text{H}^{13}\text{CO}_3^-$  have been described as an alternative method to atmospheric  $^{13}\text{CO}_2$  used to determine the production and fate of recently fixed photosynthate in trees [23]. Stem injections of  $^{13}\text{C}$ -organic acids like aspartic acid have been used to probe above-below ground carbon exchange [24]. However, there is a general lack of studies in trees reporting stem injections of respiratory substrates like sugars and alternative respiratory substrates like  $\text{C}_1$  (formate) and  $\text{C}_2$  (acetate) carboxylic acids with parallel studies on transport and canopy leaf respiratory processes. Moreover, injection studies typically perform rapid

'pulse' injections at one or several points in time with high concentrations of  $^{13}\text{C}$ -labeled substrates delivered over a short period of time. Continuous flow-controlled injections of  $^{13}\text{C}$ -labeled central plant metabolites would allow for quantitative *in-situ* studies of their fates in plants including transport and integration into specific biochemical pathways and their biological and environmental dependencies.

Here, we present a simple, programmable, xylem solution injection system which can be used for continuous diurnal injections with controlled liquid injection flow rates. We demonstrate this dynamic xylem solution injection (DXSI) technique with 1.0 L xylem injections of 10–50 mM [ $^{13}\text{C}$ ]formate and [ $^{13}\text{C}_2$ ]acetate solutions into the stem base of 2-year old potted poplar plants under controlled daytime lighting together with continuous branch gas exchange measurements in the canopy of transpiration, net photosynthesis, isoprene emissions, and  $\delta^{13}\text{CO}_2$ . These whole tree results are compared with leaf gas exchange observations on detached poplar branches pretreated with 10 mM [ $^{13}\text{C}$ ]formate and [ $^{13}\text{C}_2$ ]acetate solutions and subjected to repeated light-dark cycles under controlled environmental conditions. The results are discussed in terms of the different timescales of formate and acetate metabolism in the transpiration stream of poplar trees and the apparent impact of light on regulating acetate allocation in leaves towards respiratory versus anabolic metabolism.

## Results

Acetate delivery to detached poplar branches (*Populus trichocarpa*) via the transpiration stream enhanced leaf concentrations of TCA cycle intermediates and jasmonates (**Figure. 1**). Relative to water fed controls, acetate fed poplar branches showed large increases in TCA cycle intermediates citric acid (301 +/- 192%), succinic acid (180 +/- 56%), and  $\alpha$ -ketoglutaric acid (725 +/- 652%). Moreover, leaf concentrations of the phytohormone dihydrojasmonic acid also showed strong increases in acetate treated leaves (882 +/- 455%). This is consistent with the role of acetate in integrating into the TCA cycle and activating the jasmonate signaling pathway via protein acetylation [7]. In order to evaluate *in vivo* leaf respiratory activity,  $^{13}\text{C}$ -labeling of leaf respiratory  $\text{CO}_2$  in poplar leaves was achieved by delivery of [ $^{13}\text{C}$ ]formate and [ $^{13}\text{C}_2$ ]acetate solutions to whole trees using the Dynamic Xylem Solution Injection (DXSI) system (Fig. 2a) and detached branches placed in the respective solutions (Fig. 2b).

## Dynamic Xylem Solution Injection (DXSI) system for continuous whole tree injections of [ $^{13}\text{C}_2$ ]acetate and [ $^{13}\text{C}$ ]formate

The DXSI system was installed in the stem of individual potted poplar trees transferred from the greenhouse to the laboratory under automated soil watering and controlled lighting conditions (Fig. 3). The DXSI experiments were used to quantify diurnal transport and oxidation patterns of  $\text{C}_1$  and  $\text{C}_2$  organic acids as alternative respiratory substrates in the transpiration stream of poplar trees together with leaf respiratory metabolism via dynamic branch gas exchange observations of transpiration, net

photosynthesis, isoprene emissions, and  $\delta^{13}\text{CO}_2$ . The higher solution injection flow rate into the xylem during the day ( $150 \mu\text{L min}^{-1}$ ) compared with the night ( $70 \mu\text{L min}^{-1}$ ) was based on the observations of a strong circadian pattern in branch stomatal conductance and transpiration patterns. Non-zero elevated branch transpiration values occurred at night associated with the lack of complete stomatal closure in the dark. However, transpiration increased during the day together with net photosynthesis and isoprene emissions reaching maximum values around mid-day (Fig. 4a). Stem base injection of 10 mM  $[\text{C}_2^{13}\text{C}_2]$ acetate started in the day around 11:00 AM and induced an overall pattern of canopy branch headspace  $^{13}\text{CO}_2$  enrichment over the next 7 days. Starting with a  $\delta^{13}\text{CO}_2$  value of the reference air entering the branch enclosure ( $-7.0\text{‰}$  to  $-10.0\text{‰}$ ) a strong  $^{13}\text{C}$ -enrichment in headspace  $\text{CO}_2$  could be detected on the first day following the initiation of the xylem injections. However, despite the decrease in transpiration rates during night 1,  $\delta^{13}\text{CO}_2$  values continued to increase in the dark, reaching a maximum around  $0\text{‰}$  around midnight. Upon the light switching on the following day, branch transpiration increased together with a marked suppression in daytime  $\delta^{13}\text{CO}_2$  which rapidly increased by  $+7.0\text{‰}$  (from  $+1.0\text{‰}$  to  $+8.0\text{‰}$ ) upon darkening. While there was an overall pattern of  $^{13}\text{C}$ -enrichment in  $\text{CO}_2$  over the next 6-days ( $\delta^{13}\text{CO}_2$  up to  $+27\text{‰}$ ), the same pattern emerged with a strong diurnal structure in  $\delta^{13}\text{CO}_2$  reaching a mid-day minimum following by a maximum shortly after darkening where  $\delta^{13}\text{CO}_2$  values rapidly increased by up to  $12\text{‰}$ . Therefore, branch headspace  $\delta^{13}\text{CO}_2$  was enhanced at night and suppressed during the day, despite the higher transpiration rates during the day.

In contrast to DXSI  $^{13}\text{C}$ -labeling with a 10.0 mM solution of  $[\text{C}_2^{13}\text{C}_2]$ acetate, injection of a 10 mM  $[\text{C}^{13}\text{C}]$ formate solution into the xylem of poplar trees resulted in only small  $^{13}\text{C}$ -labeling of headspace  $\text{CO}_2$  of canopy branches (Supplementary **Figure S1**). Canopy branch transpiration, net photosynthesis, and isoprene emissions showed strong diurnal patterns with a mid-day maximum. Branch headspace  $\delta^{13}\text{CO}_2$  values of the reference air entering the branch enclosure ( $-9.0\text{‰}$  to  $-10.0\text{‰}$ ) showed only small  $^{13}\text{C}$ -enrichment on the first day ( $-3$  to  $-5\text{‰}$ ) following the initiation of the  $[\text{C}^{13}\text{C}]$ -formate xylem injections. Maximum  $\delta^{13}\text{CO}_2$  values reached around  $-5.5\text{‰}$  on mid-day of the first day, together with transpiration, net photosynthesis, and isoprene emissions. In contrast to the  $[\text{C}_2^{13}\text{C}_2]$ acetate injections, injection of a 10 mM  $[\text{C}^{13}\text{C}]$ formate solution did not result in strong and rapid enhancements in  $\delta^{13}\text{CO}_2$  upon darkening. In general,  $\delta^{13}\text{CO}_2$  declined slightly with transpiration during the night, and increased slightly during the day. The highest value of  $\delta^{13}\text{CO}_2$  was approximately  $-5.0\text{‰}$  occurring around mid-day of day 3.

In order to increase the  $^{13}\text{C}$ -labeling of  $\text{CO}_2$  during the DXSI experiments with  $[\text{C}^{13}\text{C}]$ formate xylem injections to a more comparable level to with those observed under 10 mM  $[\text{C}_2^{13}\text{C}_2]$ acetate injections, a DXSI experiment was performed starting with 10 mM  $[\text{C}^{13}\text{C}]$ formate injections for one week followed by a switch to 50 mM  $[\text{C}^{13}\text{C}]$ formate injections for an additional 4 days (supplementary **Figure S2**). Similar to the first tree injected with 10 mM  $[\text{C}^{13}\text{C}]$ formate injections for one week, headspace  $\text{CO}_2$  showed only small

$^{13}\text{C}$ -enrichment, with  $\delta^{13}\text{CO}_2$  remaining below 0.0‰ and showing maximum values during the day when transpiration was higher. Upon switching from the 10 mM [ $^{13}\text{C}$ ]formate solution to the 50 mM [ $^{13}\text{C}$ ]formate solution around midday on the 8th day, the magnitude of the diurnal increase in  $\delta^{13}\text{CO}_2$  were enhanced, reaching a maximum values of + 20.0‰ around mid-day. These values are more comparable with those observed in the 10 mM [ $^{13}\text{C}_2$ ]acetate injections. Despite the larger amplitude of day-night differences,  $\delta^{13}\text{CO}_2$  still followed diurnal patterns of transpiration, and did not show strong enhancements following darkening as observed in 10 mM [ $^{13}\text{C}_2$ ]acetate DXSI experiments. When only a 50 mM [ $^{13}\text{C}$ ]formate solution was used in a separate DXSI experiment, similar results were obtained with  $\delta^{13}\text{CO}_2$  generally following diurnal patterns of transpiration without a large increase following darkening at the beginning of the night period (Fig. 3b).

## Light-dependence of headspace $\delta^{13}\text{CO}_2$ of [ $^{13}\text{C}_2$ ]acetate and [ $^{13}\text{C}$ ]formate treated detached poplar branches

In order to further evaluate the role of light on the oxidation of acetate and formate in the transpiration stream to  $\text{CO}_2$  in leaves, leaf gas exchange in the light under controlled environmental conditions was quantified from detached branches pretreated with 10 mM [ $^{13}\text{C}_2$ ]acetate (Fig. 5a) or [ $^{13}\text{C}$ ]formate (Fig. 5b). Detached branches pretreated with 10.0 mM [ $^{13}\text{C}_2$ ]acetate in the light (Fig. 5a) showed similar levels of leaf headspace  $^{13}\text{CO}_2$ -enrichment ( $\delta^{13}\text{CO}_2$  up to + 20.0‰) to that of the whole plant DXSI experiment with 10.0 mM [ $^{13}\text{C}_2$ ]acetate injections where the dynamic branch headspace  $\delta^{13}\text{CO}_2$  values reached up to 20.0‰ during the day. Moreover, the strong  $^{13}\text{CO}_2$ -enrichment in the dynamic leaf headspace atmosphere, as measured in real time by CRDS, was confirmed using grab samples collected manually and analyzed offline using IRMS. Throughout the 4-hour experiment in the light, net photosynthesis, stomatal conductance, and transpiration slightly decreased, but maintained values typical of a physiologically active mature poplar leaves in the light. In contrast to the whole plant DXSI injections with 10 mM [ $^{13}\text{C}$ ]formate, which resulted in only small  $^{13}\text{C}$ -labeling of headspace  $\text{CO}_2$  of canopy branches, detached branches pretreated with 10.0 mM [ $^{13}\text{C}$ ]formate in the light showed much higher levels of leaf headspace  $^{13}\text{CO}_2$ -enrichment ( $\delta^{13}\text{CO}_2$  up to + 322‰) (Fig. 5b). Throughout the 4-hour experiment in the light, net photosynthesis, stomatal conductance, and transpiration maintained high values representative of highly physiologically active mature poplar leaves in the light. In summary, leaf  $\delta^{13}\text{CO}_2$  values in 10.0 mM [ $^{13}\text{C}_2$ ]acetate treated branches in the light reached similar values as branches of intact poplar trees during DXSI experiments with 10.0 mM [ $^{13}\text{C}_2$ ]acetate injected into the xylem. In contrast, leaf  $\delta^{13}\text{CO}_2$  values in 10.0 mM [ $^{13}\text{C}$ ]formate treated branches in the light far exceeded values from canopy branches during DXSI experiments with 10.0 mM [ $^{13}\text{C}$ ]formate injected into the xylem.

To evaluate the role of light on leaf  $^{13}\text{CO}_2$  production from  $[^{13}\text{C}_2]$ acetate oxidation via mitochondrial respiration, a leaf from a branch pretreated with 10.0 mM  $[^{13}\text{C}_2]$ acetate was placed in the dynamic leaf chamber in the light and subjected to three sequential light-dark and dark-light transitions under controlled environmental conditions. Leaf headspace  $\delta^{13}\text{CO}_2$  on branches pretreated with 10.0 mM  $[^{13}\text{C}_2]$ acetate showed a rapid and strong response to repeated light-dark and dark-light cycles (Fig. 6). Consistent with the whole plant and branch gas exchange studies, switching the light off at the leaf level induced a rapid increase in  $\delta^{13}\text{CO}_2$  by up to +70‰ within 6 min after darkening. Upon switching the light back on,  $\delta^{13}\text{CO}_2$  rapidly decreased by -45‰ within 6 min after re-illumination, and thereafter decreased more slowly to return to close to the initial  $\delta^{13}\text{CO}_2$  value after 30 min. Three sequential dark-light and light-dark cycles showed similar results, demonstrating the reversibility of the apparent light-inhibition of  $[^{13}\text{C}_2]$ acetate respiration (Fig. 6).

## Discussion

Introduction of solutions into plants and trees have long been of interest to farmers, forest managers, land owners, and researchers with injections directly into the conductive tissues of trees first investigated systematically by Leonardo da Vinci [25]. Direct injections avoid some of the negative aspects of normal external delivery methods such as sprays and soil additions which are sometimes ineffective and wasteful with extensive evaporation and runoff leading to unwanted side effects from alterations in soil microbial metabolism to damaging the local environment through toxic effects [26]. Motivated by insect [27] and microbial-linked [28] epidemics responsible for widespread tree mortality events [29], several xylem injection methods have been described including trunk infusion and pressurized trunk injections [30]. With infusion, chemical solutions are contained in a reservoir and interfaced into a tree trunk with tubing and a needle such that the solution slowly (over days) flows down into the trunk [31]. The advantage of this method is the simplicity of the setup and minimal damage to the tree, although issues have been described including difficulty of use, long infusion times and low flow rates (e.g. 300 mL after 14 days), and troubleshooting including low to no apparent uptake of the solution [32]. Stem infusions (passive from intravenous bags) or injections via a syringe or port delivered actively from pressurized containers have become a common method for delivery of bioactive defense substances to trees and shrubs as an environmental friendly way of controlling biological stress from bacteria, fungi, nematodes, and insects [26]. Simple stem infusion and injection techniques have successfully been used for plant protection against biotic stress and disease management against microbes including bacteria and fungi as well as insects [33].

However, one major disadvantage of the infusion method is that the injection flow rates are low, not constant (decreases with time), and are largely unknown. To get around the slow injection rates, in 1976, a “portable pressure-injection machine” was described as an effective means of treating pear trees for pear decline with antibiotics and consisted of compressed air/ $\text{N}_2$ , a liquid reservoir, an injection needle with a feed tube, and a valve [34]. This system, which is now commercially available from numerous

manufacturers, allows for the rapid injections of small (few ml) to high volumes of solution (few L). Annual stem injections of the fungus *Verticillium albo-atrum*, which activates natural defense mechanisms, have been used to greatly reduce the incidence of Dutch Elm Disease (DED) caused by the fungus *Ophiostoma ulmi* (Buisman) Nannfeldt. Since 2010 in the Netherlands, only 0.5% of the injected elms became infected with DED [35]. In addition to defense related compounds against biotic stress, stem injections have also been used to deliver numerous other substances including fertilizers [36, 37] and phytohormonal plant growth regulators [38]. Many of these have shown promising results from traditional crop spraying techniques that act as blossom and postbloom thinners, regulators of plant development and maintenance of optimal tree structure, vegetative growth control, flowering and fruit set, improving fruit appearance, and fruit maturity and quality [39]. For example, when the phytohormone salicylic acid was injected together with sucrose into corn plants, grain yield increased by 9% and net photosynthetic rates were reported as high as 42% relative to the injection of distilled water [38].

By controlling the injection flow rate into the xylem of 2-year old poplar trees at low values (e.g. 70–150  $\mu\text{L min}^{-1}$ ), the presented DXSI injection method allows for continuous injections of solutions with programmable delivery rates such that high volumes (e.g. L) of solution can be injected over longer periods of time. Thus, the developed DXSI method presented here has features of both the infusion method (low flow rates delivered over longer time periods) and the injection method (direct injection of liquid solutions into the xylem) and is therefore ideal for quantitative studies of leaf day respiration using isotopically labeled substances. While we held DXSI injection flow rates constant during the day and night, a circadian rhythm of transpiration and stomatal conductance was observed, despite constant environmental conditions. Thus, we suggest future improvements of the DXSI method to continuously scale injection flow rates with sap flow rates. This would, in theory, enable a constant concentration of injected substances in the xylem sap, regardless of the sap velocity. Thus, the DXSI method is anticipated to be useful as a continuous injection technique allowing the observation of diurnal patterns not typically resolved by rapid pulse-injection experiments. While we used  $^{13}\text{C}$ -solutions for isotopic labeling, this technique could also be applied to plant hormones and other biologically active substances where continuous injections of low concentrations would be useful for studying transport, metabolism, and biological impacts. In addition to  $^{13}\text{C}$ -labeled respiratory substrates described here, another promising avenue is the partitioning of net leaf  $\text{O}_2$  fluxes in the light into gross  $\text{O}_2$  fluxes associated day respiration, photorespiration and photosynthesis in leaves by combining the DXSI technique with  $\text{H}_2^{18}\text{O}$  xylem injections and leaf oxygen flux and  $\delta^{18}\text{O}_2$  measurements [40].

## Transport and metabolism of $\text{C}_1$ and $\text{C}_2$ organic acids in detached branches and whole trees

Numerous analytical methods are currently being explored in the study of leaf day respiration and the apparent suppression effects of light [15]. The two main approaches used to estimate leaf day respiration rates are the Loreto  $^{13}\text{CO}_2$  isotopic method [41] and the Kok method [11]. The Loreto method

assumes that in an atmosphere of  $^{13}\text{CO}_2$ , all  $^{12}\text{CO}_2$  detected is from respiration, and is considered to be the most accurate method [15]. The Kok method uses the abrupt change in the initial slope of the response of net photosynthesis to irradiance at low light (*i.e.* sudden change in the quantum yield of photosynthesis near the light compensation point) [42];[16];[11]. Studies using stable isotope tracing have demonstrated important insights when combined with real-time gas exchange and leaf physiological measurements. For example, leaf labeling with  $^{13}\text{CO}_2$  in the atmosphere and [ $^{13}\text{C}$ ]glucose and [ $^{13}\text{C}$ ]pyruvate leaf feeding have provided strong evidence for the reversible inhibition of respiratory enzymes in illuminated leaves [15, 18, 43]. For instance, [ $^{13}\text{C}$ ]glucose was previously shown to be blocked in the light from entering glycolysis and instead diverted to sucrose synthesis [44]. More recently leaf [ $^{13}\text{C}$ ]glucose decarboxylations have been quantified as low, but significant in the light, and increase with decreasing irradiance below  $100 \mu\text{mol photons m}^{-1} \text{s}^{-1}$  [18]. Moreover, while TCA cycle decarboxylations of [ $^{13}\text{C}$ ]pyruvate is strongly light-inhibited (e.g. 80–95%), mitochondrial PDH decarboxylating activity has been shown to be only ~ 30% inhibited in the light relative to the dark [44, 45]. Thus, the strong suppression of TCA cycle decarboxylations in the light may be related to the strong light inhibition of other TCA cycle enzymes such as citrate synthase (CS), which condenses acetyl-CoA with oxaloacetate as the first step of the TCA cycle in mitochondria [15].

While light inhibition of CS has been demonstrated [19], its role in the light suppression of leaf day respiration remains under investigation. In this study, we bypassed formation of acetyl-CoA via the mitochondrial PDH reaction, by supplying [ $^{13}\text{C}_2$ ]acetate via the transpiration stream in detached branches and whole trees using a new developed method termed Dynamic Xylem Solution Injection (DXSI). Given that formate oxidation to  $\text{CO}_2$  as a part of the  $\text{C}_1$  pathway in plants does not involve TCA cycle enzymes [5], we used both detached branch labeling and whole tree DXSI labeling with [ $^{13}\text{C}$ ]formate to contrast with [ $^{13}\text{C}_2$ ]acetate transport and light-dependent metabolism in poplar trees. The similar  $^{13}\text{C}$ -enrichment of headspace  $\text{CO}_2$  in the whole plant DXSI (Fig. 4a) and detached branch (Fig. 5a) labeling experiments with 10 mM [ $^{13}\text{C}_2$ ]acetate suggests that acetate is efficiently transported in the xylem to leaf cells where it is utilized as a respiratory substrate. However, within minutes of switching off the grow light at the start of each night period during the whole tree DXSI studies (Fig. 4a), or the light source within the leaf chamber during the detached branch studies (Fig. 6),  $\delta^{13}\text{CO}_2$  values rapidly increased. Upon switching the light back on in the morning for the whole tree DXSI experiment or after ~ 30 minutes of darkness during the detached branch/leaf studies,  $\delta^{13}\text{CO}_2$  values rapidly decreased, returning to similar values in the previous light period. These observations demonstrate that the light inhibition of leaf  $^{13}\text{CO}_2$  efflux during [ $^{13}\text{C}_2$ ]acetate labeling is reversible.

The results demonstrate that acetate in the transpiration stream is an effective respiratory substrate. However, before acetate can be utilized as a respiratory substrate in mitochondria, it must first be activated to acetyl-CoA. As acetyl-CoA is membrane impermeable, the use of acetate as a respiratory substrate is assumed to require acetate activation to acetyl-CoA within mitochondria. While acetate is

known to be activated to acetyl-CoA in peroxisomes and chloroplasts through the reaction catalyzed by an acetyl-CoA synthetase localized to those organelles [46], a mitochondrial acetyl-CoA synthetase has not been clearly demonstrated in plants like it has in animals [47]. Another potential mechanism for acetate utilization in mitochondrial respiration is the glyoxylate cycle, which starts in peroxisomes and depends on mitochondrial TCA cycle metabolism, providing plants the ability to convert C<sub>2</sub> acetate to C<sub>4</sub> respiratory substrates like citrate, isocitrate, glyoxylate, malate, and oxaloacetate which can be used to replenish the TCA cycle or as precursors for amino acid or sugar biosynthesis [48]. The glyoxylate cycle in seeds is known for its important roles in converting storage lipids to sugars through the integrated activities of β-oxidation, the glyoxylate and TCA cycles, and gluconeogenesis [49]. In contrast, relatively less is known about the function of the glyoxylate cycle in leaves including its integration with fermentation, photosynthesis, photorespiration, and mitochondrial respiration. However, *Arabidopsis thaliana* mutant seedlings which lack the glyoxylate cycle are completely unable to convert acetate into sugar and show a dramatic decrease in the frequency of seedling establishment and compromised growth in low light or reduced daylength conditions [50]. In the case where acetate can be activated to acetyl-CoA directly within mitochondria, the observations of a rapid and strong enhancement in leaf <sup>13</sup>CO<sub>2</sub> efflux upon darkening during [<sup>13</sup>C<sub>2</sub>]acetate labeling may be related to the dark activation of mitochondrial CS [19]. Similarly, in the case where acetate is activated to acetyl-CoA within peroxisomes as a part of the glyoxylate cycle, peroxisomal CS may also be strongly dark activated. Recent studies with the photosynthetic green alga *Chlamydomonas reinhardtii* demonstrate that not only do the abundances of enzymes involved in the glyoxylate cycle become elevated under heterotrophic conditions (dark and in the presence of external acetate), peroxisomal CS activity dramatically increases via protein acetylation [51]. Nonetheless, it is important to note that other mechanisms could also be at play, and lead to a similar “apparent” suppression of [<sup>13</sup>C<sub>2</sub>]acetate respiration in the light including the re-assimilation of respiratory <sup>13</sup>CO<sub>2</sub> by photosynthesis [12]. However, in contrast to whole [<sup>13</sup>C<sub>2</sub>]acetate labeling, DXSI experiments with 10 and 50 mM [<sup>13</sup>C]formate did not show strong enhancements in δ<sup>13</sup>CO<sub>2</sub> branch efflux upon darkening at night (Fig. 4b and supplementary **Figures S1-S2**). This implies that re-assimilation of respiratory <sup>13</sup>CO<sub>2</sub> by photosynthesis may not explain the strong dark enhancement in δ<sup>13</sup>CO<sub>2</sub> observed during [<sup>13</sup>C<sub>2</sub>]acetate labeling. Nonetheless, the metabolic pathway(s) of [<sup>13</sup>C<sub>2</sub>]acetate oxidation to <sup>13</sup>CO<sub>2</sub> including the subcellular location of activation to acetyl-CoA, potential involvement of the glyoxylate cycle in integrating acetate metabolism with the TCA cycle, light inhibition of TCA and glyoxylate cycle enzymes including CS, and the role of re-assimilation of respiratory <sup>13</sup>CO<sub>2</sub> by photosynthesis requires further research to resolve.

Supplying 10 mM [<sup>13</sup>C<sub>2</sub>]acetate to detached branches and whole trees during DXSI injections showed similar <sup>13</sup>C-enrichments in leaf and branch headspace δ<sup>13</sup>CO<sub>2</sub>, respectively. In contrast, detached branch labeling with 10 mM [<sup>13</sup>C]formate resulted in much higher values of leaf headspace δ<sup>13</sup>CO<sub>2</sub> compared with branch headspace δ<sup>13</sup>CO<sub>2</sub> during 10 mM [<sup>13</sup>C]formate whole tree DXSI experiments (Fig. 5b vs **supplementary Figure S1**). This suggests that formate is rapidly oxidized to CO<sub>2</sub> within the transpiration

stream, likely catalyzed by formate dehydrogenase enzymes localized to both mitochondria and chloroplasts in higher plants [6]. During whole plant DXSI labeling experiments, a 50 mM [ $^{13}\text{C}$ ]formate solution was required to reach similar levels of canopy branch  $\delta^{13}\text{CO}_2$  as 10 mM [ $^{13}\text{C}_2$ ]acetate (Fig. 4b vs Fig. 4a). These observations suggest that formate has a shorter lifetime within the transpiration stream of poplar relative to acetate, such that by the time the solution reaches the canopy leaves, the majority of the [ $^{13}\text{C}$ ]formate has already been oxidized to  $^{13}\text{CO}_2$ . Moreover, relative to acetate, formate did not show indications of a strong light-inhibition of oxidation to  $^{13}\text{CO}_2$ . This is consistent with the observations that  $\delta^{13}\text{CO}_2$  during DXSI delivery of 10 and 50 mM [ $^{13}\text{C}$ ]formate generally showed maximum values in the light during the day when delivery rates of [ $^{13}\text{C}$ ]formate to leaves via the transpiration stream was higher. In contrast, branch headspace  $\delta^{13}\text{CO}_2$  values during DXSI experiments with [ $^{13}\text{C}_2$ ]acetate generally showed minimum values during the day (Fig. 4a). These observations show the utility of combining labeling of detached branches with high environmental control over leaf gas exchange conditions such as light during short-term experiments over hours with whole tree DXSI experiments over longer time scales (e.g. days to months) to characterize the transport and metabolism of respiratory intermediates from small (leaf to branch) to larger (stem and canopy) scales. Thus, reducing the need for destructive sampling, long-term DXSI experiments with  $^{13}\text{C}$ -labeled respiratory substrates are anticipated to be a useful tool in the investigation of quantitative day and night leaf respiratory processes including its integration with other major primary metabolic pathways including fermentation, photosynthesis, photorespiration, and the glyoxylate cycle.

## Conclusions

Acetate fermentation has recently been demonstrated as a key mechanism of drought survival through the signaling properties of acetate including protein acetylation, with the amount of acetate produced directly correlating to survival. While the defense signaling properties of acetate have been the focus of previous studies via protein acetylation, here we demonstrate the potential for acetate in the transpiration stream of trees to be utilized as a respiratory substrate. The dynamic xylem solution injection method (DXSI) presented here allows for continuous injections of isotopically labeled metabolite solutions with programmable injection rates such that diurnal patterns of metabolic activity can be studied including differences in carbon allocation patterns during the day and night. The DXSI method has features of both the infusion method (low flow rates delivered over longer time periods) and the injection method (direct injection of liquid solutions into the xylem) and is therefore ideal for quantitative studies of leaf day respiration using isotopically labeled substances. While the majority of studies investigating day respiration in plants using isotopic labeling methods have employed common respiratory substrates during short duration labeling experiments with detached leaves (e.g. [ $^{13}\text{C}_{1-6}$ ]glucose and [ $^{13}\text{C}_{1-3}$ ]pyruvate), we show that the alternative  $\text{C}_1$  and  $\text{C}_2$  respiratory substrates [ $^{13}\text{C}_2$ ]acetate and [ $^{13}\text{C}$ ]formate are oxidized to  $^{13}\text{CO}_2$  within intact poplar trees with distinct differences in their rates of oxidation to  $^{13}\text{CO}_2$  and light influence. [ $^{13}\text{C}$ ]formate is rapidly converted to  $^{13}\text{CO}_2$  during transport in the

transpiration stream, with  $^{13}\text{CO}_2$  efflux from canopy leaves increasing with transpiration during the day. In contrast,  $[^{13}\text{C}_2]$ acetate is efficiently transported to canopy leaves with a strong enhancement in leaf  $^{13}\text{CO}_2$  efflux at night when transpiration is reduced. Leaf gas-exchange experiments on detached branches pre-treated with  $[^{13}\text{C}_2]$ acetate in the light confirm the strong and reversible apparent light inhibition of  $[^{13}\text{C}_2]$ acetate respiration. While acetate may not be able to directly enter the TCA cycle due to the potential lack of a mitochondrial acetyl-CoA synthetase, the results are consistent with the well characterized peroxisomal acetyl-CoA synthetase effectively integrating acetate into the glyoxylate cycle which is dependent on TCA cycle activity. The strong apparent suppression of  $[^{13}\text{C}_2]$ acetate respiration in the light cannot be explained by the well-known inhibition of mitochondrial PDH, and instead may be related to the light inhibition of mitochondrial or peroxisomal CS. The results highlight the potential for an effective integration of acetate into the glyoxylate and TCA cycles and the light-inhibition of CS as an important regulatory mechanism in controlling the diurnal allocation of acetate between anabolic and catabolic processes.

## Materials And Methods

### Plant material

Poplar (black cottonwood: *Populus trichocarpa*) saplings were obtained from Plants of the Wild (Washington State, USA). The two-year old trees were maintained at the UC Berkeley Oxford Tract greenhouse, grown in super soil media (Scotts Co., Marysville, Ohio, USA) within 5-gallon pots with automated watering. Natural sunlight was supplied and supplemented with additional LED lighting (Lumigrow 325 Pro, California, USA) controlled using an application controller with photocell (Argus Titan, British Columbia, Canada). The controller was programmed to turn LED lights off when detecting exterior light levels above  $850 \mu\text{mol m}^{-2} \text{s}^{-1}$  during the 16-hour photoperiod (6AM to 10PM).

### Relative quantification of leaf TCA cycle and jasmonate in acetate treated leaves

In order to assess the role of acetate on leaf respiration and defense signaling, detached poplar branch feeding with 10 mM acetate solutions were used to characterize acetate-induced changes in leaf TCA cycle intermediates (respiration) and jasmonates (signaling and defense) concentrations. Detached poplar branches were placed in water ( $n = 3$ ) or 10 mM acetate ( $n = 3$ ) for 24 hours in a humidified growth chamber (RH: 90–95%) and recut under the solution to prevent excess air from entering and disrupting the transpiration stem of the branch. The detached branch in the solutions was maintained in a growth chamber (Percival Intellus Control System, Perry, Iowa, USA) with daytime settings of 27.5°C, 30% light (6:00AM-8:00PM) and 25°C, 0% light during the night (8:00PM-6:00AM). One leaf from the water control (3) and acetate treated branches (3) were extracted, dried, resuspended in 80:20 methanol:water and analyzed for TCA cycle and jasmonate metabolite levels. Compounds were separated using Thermo Hypersil GOLD (2.1 × 150 mm length, 3  $\mu\text{m}$  particle size) with a 2.1 mm, 0.2  $\mu\text{m}$  filter cartridge, column

temperature set to 40 °C and a flow rate of 400  $\mu\text{L min}^{-1}$ . Mobile phase A (0.1% Formic acid in H<sub>2</sub>O) and B (0.1% Formic acid in ACN) were initially 90:10 respectively. The gradient continued as follows: 0–2 min 90% A; 2–11 min 10% A; 11–12 min held at 10% A; 12–12.5 min 10% A; 12.5–13.5 min 90% A with an increased flow rate of 500  $\mu\text{L min}^{-1}$ ; 13.5–14 min 90% A; 14–14.5 min 90% A with a decreased flow rate of 400  $\mu\text{L min}^{-1}$ ; 14.5–15 min held at 90% A. RP LC-MS (Reverse-Phase Liquid Chromatography Mass Spectrometry). Data-dependent acquisition was acquired on a Thermo Qexactive Orbitrap mass spectrometer with a scan range of 80 to 800 m/z. Thermo Raw files were processed using MZmine 2 and exported as csv. Citric acid (1.04 min retention time), succinic acid (1.26 min retention time), and  $\alpha$ -ketoglutaric acid (1.19 min retention time) were identified and verified using retention time, monoisotopic mass, and MS<sup>2</sup> match to internal database. Dihydrojasmonic acid (7.74 min retention time) was identified using only retention time and monoisotopic mass match to internal database.

## Dynamic Xylem Solution Injection (DXSI) system

The DXSI system consists of a liquid handling pump interfaced with the solution reservoir (pump input) and the xylem of a poplar tree (pump output) through 1/16" outer diameter tubing. For each of the four trees studied, they were first transported before sunrise from the UC Berkeley Oxford greenhouse to the nearby analytical laboratory (Lawrence Berkeley National Laboratory) and placed under an LED grow light (90 W Baisheng Semiconductor Lighting Co., Ltd.) supplying 400–1000  $\mu\text{mol m}^{-2} \text{s}^{-1}$  photosynthetically active radiation intensity at the top of the tree canopy during the daytime (6:00–18:00). A single automated watering system was used to deliver water (~ 200 mL in 10 seconds) to the soil of the potted tree every 3 hours. Prior to the initiation of the light period, two 1/16" silcosteel tubes (1/16" outer diameter and 0.04" inner diameter, Restek Inc.) containing the solution to be injected were installed into the xylem of the tree. A 1/16" diameter hole was drilled 2.5 cm deep at a 45-degree angle (with respect to horizontal) approximately 15 cm above the soil surface. Immediately following this, a second hole 18 cm above the soil surface on the opposite side of the first hole was created with the same method. The two 1/16" tubes containing the <sup>13</sup>C-labeled solution were each inserted 2.5 cm deep directly into the drilled holes and sealed at the surface of the stem using 10 sequential layers of Loctite epoxy adhesive with Loctite adhesive accelerator (Loctite 380 adhesive; Loctite 712 adhesive accelerator, Henkel Corporation, CT, USA). Prior to installation, the silcosteel tubes were each gently bent into a half-circle shape, such that the metal tubing could be inserted into opposite sides of the poplar tree stem, allowing for fluid injection into two locations in the xylem. The two silcosteel tubes were connected together with an 1/16" stainless steel tee which was connected to the output of a programmable liquid handling pump (M6 M Series Pump, Valco Instruments Co. Inc., USA) via a 1/16" Teflon tube. This setup allowed for the liquid flow from the M6 pump to be diverted to both xylem injection points. Prior to installation of the silcosteel tubes into the xylem, the liquid pump and tubing were flushed with the <sup>13</sup>C-solution overnight (50  $\mu\text{L min}^{-1}$  x 8–10 hours).

Over 7 days, 1.0 L solutions of 10.0 mM Na-[<sup>13</sup>C<sub>2</sub>]acetate or 10–50 mM Na-[<sup>13</sup>C]formate were placed in the M6 Pump's supply reservoir and solution output dispensing volumetric flow rates were programmed

using the Mforce controller application (VICI-Valco Instruments)). A diurnal dispensing method was used, with a constant xylem injection flow rate of  $70 \mu\text{L min}^{-1}$  during the night (8:00 PM to 6:00 AM) and  $150 \mu\text{L min}^{-1}$  during the day (6:00 AM to 8:00 PM).

## Detached branch labeling

In order to compare whole tree responses to [ $^{13}\text{C}$ ]formate and [ $^{13}\text{C}_2$ ]acetate xylem solution injections, detached branch solution labeling studies were also performed with leaf gas exchange measurements conducted under constant daytime environmental conditions. Poplar trees were obtained from the greenhouse (Oxford Tract Farm, UC Berkeley) before sunrise and transported to the analytical laboratory. A 30 cm branch was cut from the poplar tree and immediately immersed into a 250 mL flask of solution (10 mM [ $^{13}\text{C}_2$ ]acetate or 10 mM [ $^{13}\text{C}$ ]formate) and recut under the solution to prevent excess air from entering and disrupting the transpiration stem of the branch. The detached branch in the solutions was maintained in a growth chamber (Percival Intellus Control System, Perry, Iowa, USA) with daytime settings of  $27.5^\circ\text{C}$ , 30% light (6:00 AM-8:00 PM) and  $25^\circ\text{C}$ , 0% light during the night (8:00 PM-6:00 AM) for one day (10–16 hours) prior to leaf gas exchange measurements.

## Gas exchange analysis

In order to evaluate the impact of the xylem solution injections on leaf gas exchange, a dynamic 5.0 L Tedlar branch enclosure (5 Liter Tedlar Bag, CEL Scientific Corporation, USA) was installed on one of the branches near the top of the tree. Gas exchange analysis was performed by enclosing a branch with 5–10 leaves inside the enclosure with  $2.0 \text{ L min}^{-1}$  hydrocarbon free air continuously passing through. The air contained ambient levels of  $\text{CO}_2$  and  $\text{H}_2\text{O}$ , with trace volatile organic compounds (VOCs) removed by catalytic oxidation at  $400^\circ\text{C}$  (737 pure air generator, Aadco Instruments Inc, USA). The enclosure was secured around the stem at the base with air entering the top through the  $\frac{1}{4}$ " valve port and venting at the bottom where the enclosure was secured to the stem ( $1,775 \text{ mL min}^{-1}$ ), with  $225 \text{ mL min}^{-1}$  diverted to three real-time gas sensors for quantification of **1**)  $\text{CO}_2$  and  $\text{H}_2\text{O}$  concentrations (Li7000, Li-Cor Biosciences, USA), **2**)  $^{12}\text{CO}_2$  and  $^{13}\text{CO}_2$  concentrations together with  $\delta^{13}\text{CO}_2$  (G2131-I High Precision Isotopic Carbon analyzer, Picarro Inc, USA), and **3**) isoprene concentrations via high sensitivity quadrupole Proton Transfer Reaction - Mass Spectrometer (PTR-MS, Ionicon, Austria).

The Li7000 was operated in absolute mode with the reference cell continuously provided  $100 \text{ mL min}^{-1}$  of ultra-high purity nitrogen (5.0 purity, Praxair, Danbury, CT, USA) and designated as 0 ppm  $\text{CO}_2$  and  $0 \text{ mmol mol}^{-1} \text{ H}_2\text{O}$ .  $100 \text{ mL min}^{-1}$  of air from inside the branch enclosure was directed to the Li7000 sample cell with average  $\text{CO}_2$  and  $\text{H}_2\text{O}$  concentrations recorded every minute. Branch headspace  $^{12}\text{CO}_2$  and  $^{13}\text{CO}_2$  concentrations together with  $\delta^{13}\text{CO}_2$  were analyzed using a G2131-I High Precision Cavity Ringdown Spectrometer (CRDS, Picarro Inc., USA).  $25 \text{ mL/min}$  of branch enclosure headspace air was passed first through a water trap to remove water vapor (Dririte), before passing through a particle filter (Gelman 1 Micron Filter Assembly) and entering the Isotopic  $\text{CO}_2$  analyzer. The PTR-MS was operated with a drift

tube voltage of 600 V and pressure of 1.9 mb and quantified isoprene emissions at m/z 69 as previously described [52].

For leaf gas exchange studies on detached branches pretreated with 10 mM [ $^{13}\text{C}_2$ ]acetate or [ $^{13}\text{C}$ ]formate, a portable leaf photosynthesis system was utilized (Li6800 with small light source 6800-02, Li-Cor Biosciences, Lincoln, NE, USA). The subsampling port was used to divert a small percentage of the sample flow exiting the leaf chamber to the PTR-MS and CRDS for online measurements of isoprene and  $\delta^{13}\text{CO}_2$ , respectively. The leaf chamber was operated under the following constant environmental conditions: 400  $\mu\text{mol s}^{-1}$  hydrocarbon free air flowing through the leaf chamber, 30°C leaf temperature, 420 ppm reference  $\text{CO}_2$ , and 15  $\text{mmol mol}^{-1}$  reference  $\text{H}_2\text{O}$ . For the first part of the experiment, the light was held at 1,000  $\mu\text{mol m}^{-2} \text{s}^{-1}$  photosynthetically active radiation, before cycling off (30 min) and on (30 min) three times.

For one DXSI and one leaf level experiment with 10 mM [ $^{13}\text{C}_2$ ]acetate, real-time  $\delta^{13}\text{CO}_2$  observations using CRDS were compared with grab air samples and analyzed for  $\delta^{13}\text{CO}_2$  by isotope ratio mass spectrometry (IRMS). Samples (~ 65 mL) were collected in a sterile airtight syringe and then injected into 58 mL evacuated glass vials sealed with 20 mm-thick blue chlorobutyl rubber septa (Bellco Glass, Inc., Vineland, NJ, USA). Carbon isotope ratios of  $\text{CO}_2$  were measured in 5 mL aliquots extracted with an airtight syringe and injected into Helium flushed 12 mL Labco exetainer vials. The  $\text{CO}_2$  was analyzed using a headspace autosampler (Gilson, Villiers-le-Bel, France) linked to a trace gas pre-concentrator interfaced to a Micromass JA Series Isoprime isotope ratio mass spectrometer (Micromass, Manchester, UK). The samples were transferred to a liquid nitrogen trap by flushing the Labco exetainer vial with ultra-pure He. By heating the liquid nitrogen traps, the  $\text{CO}_2$  was transferred and separated chromatographically from  $\text{N}_2\text{O}$  on a Poraplot Q fused silica capillary column (30 m x 0.32 mm), and the carbon isotope ratios were measured in the mass spectrometer. Repeated injections of a laboratory standard associated with sample analysis yield  $\delta^{13}\text{CO}_2$  values of  $-33.79 \pm 0.75\text{‰}$  ( $1\sigma$ ; n = 11).

## Abbreviations

**Acetyl-CoA:** Acetyl-Coenzyme A

**$\text{CO}_2$ :** Carbon dioxide

**CRDS:** Cavity ringdown spectroscopy

**CS:** Citrate synthase

**DED:** Dutch Elm Disease

**DXSI:** Dynamic Xylem Solution Injection

$\delta^{13}\text{CO}_2$ : Ratio of stable isotopes  $^{13}\text{CO}_2/^{12}\text{CO}_2$ , reported in parts per thousand (per mil, ‰) relative to the Pee Dee Belemnite (PDB) standard

$\text{H}_2\text{O}$ : Water

**IRMS**: Isotope ratio mass spectrometry

**LC-MS**: Liquid chromatography mass spectrometry

**LED**: Light emitting diode

**PDH**: Pyruvate dehydrogenase

**PTR-MS**: Proton transfer reaction-mass spectrometry

**TCA**: Tricarboxylic acid cycle

## Declarations

### Ethics approval and consent to participate

Not applicable.

### Consent for publication

Not applicable.

### Competing interests

The authors declare that they have no competing interests.

### Funding

This material is based upon work supported by the U.S. Department of Energy (DOE), Office of Science, Office of Biological and Environmental Research (BER), Biological System Science Division (BSSD), Early Career Research Program under Award number FP00007421 to Lawrence Berkeley National Laboratory. This work was also supported as part of the DOE Joint BioEnergy Institute through contract DE-AC02-05CH11231 to Lawrence Berkeley National Laboratory. A portion of this research was performed on project awards ([10.46936/cpcy.proj.2019.50708/60006566](#) and [10.46936/expl.proj.2019.51078/60006676](#)) from the Environmental Molecular Sciences Laboratory, a DOE Office of Science User Facility sponsored by the BER program under Contract No. DE-AC05-76RL01830.

### Acknowledgments

We would like to acknowledge extensive project guidance from Christina Wistrom for the maintenance and establishment of our poplar trees at the UC Berkeley Oxford Greenhouse and the extensive IT technical support by Bryan Taylor at the Lawrence Berkeley National Laboratory.

### **Authors' contributions**

K. Jardine designed the DXSI methodology and experimental plan with J. Mortimer, P. Handkumbura, R. Young, H. Mehta, and E. Brodie; J. Lei designed the graphical abstract and was responsible for all DXSI configurations and installations into tree stems; K. Jardine and J. Lei collected the experimental physiological data; P. Handakumbura maintained poplar trees for experimental study; M. Bill provided IRMS data and wrote the corresponding IRMS methods; C. Clendinen extracted metabolites from frozen poplar leaf samples and analyzed them for TCA cycle and jasmonate levels as a part of the Environmental Molecular Sciences Laboratory (EMSL) DOE user facility project, "Poplar esterified cell wall transformations and metabolic integration (PECTIN) study". All co-authors participated in data analysis, figure preparation, and writing of the manuscript.

### **Data availability and supplementary information**

All raw data generated during this study (PTR-MS, CRDS, IRMS, Li7000, Li6800, and LC-MS) will be included as supplementary files with the published article. In addition, the following supplementary figures are included;

**Supplementary Figure 1:** Time series of headspace  $\delta^{13}\text{CO}_2$  in a dynamic poplar branch enclosure during a DXSI experiment using a 10 mM solution of [ $^{13}\text{C}$ ]formate.

**Supplementary Figure 2:** Time series of headspace  $\delta^{13}\text{CO}_2$  in a dynamic poplar branch enclosure during a DXSI experiment using a 10 mM solution of [ $^{13}\text{C}$ ]formate which is subsequently switched to a 50 mM solution of [ $^{13}\text{C}$ ]formate.

## **References**

1. O'Leary BM, Asao S, Millar AH, Atkin OK. Core principles which explain variation in respiration across biological scales. *New Phytol.* 2019;222:670–86.
2. Vanlerberghe GC, Dahal K, Alber NA, Chadee A. Photosynthesis, respiration and growth: A carbon and energy balancing act for alternative oxidase. *Mitochondrion.* 2020;52:197–211.
3. Tovar-Méndez A, Miernyk JA, Randall DD. Regulation of pyruvate dehydrogenase complex activity in plant cells. *Eur J Biochem.* 2003;270:1043–9.
4. Florez-Sarasa I, Fernie AR, Gupta KJ. Does the alternative respiratory pathway offer protection against the adverse effects resulting from climate change? *J Exp Bot.* 2020;71:465–9.
5. Jardine KJ, Fernandes de Souza V, Oikawa P, Higuchi N, Bill M, Porras R, et al. Integration of C<sub>4</sub> and C<sub>3</sub> metabolism in trees. *Int J Mol Sci.* 2017;18:2045.

6. Herman PL, Ramberg H, Baack RD, Markwell J, Osterman JC. Formate dehydrogenase in *Arabidopsis thaliana*: overexpression and subcellular localization in leaves. *Plant Sci.* 2002;163:1137–45.
7. Kim J-M, To TK, Matsui A, Tanoi K, Kobayashi NI, Matsuda F, et al. Acetate-mediated novel survival strategy against drought in plants. *Nat Plants.* 2017;3:17097.
8. Dewhirst RA, Lei J, Afseth CA, Castanha C, Wistrom CM, Mortimer JC, et al. Are Methanol-Derived Foliar Methyl Acetate Emissions a Tracer of Acetate-Mediated Drought Survival in Plants? *Plants.* 2021;10.
9. Fletcher JS, Beevers H. Acetate metabolism in cell suspension cultures. *Plant Physiol.* 1970;45:765–72.
10. Fu X, Yang H, Pangestu F, Nikolau BJ. Failure to Maintain Acetate Homeostasis by Acetate-Activating Enzymes Impacts Plant Development. *Plant Physiol.* 2020;182:1256–71.
11. Kok B. On the interrelation of respiration and photosynthesis in green plants. *Biochimica et biophysica acta.* 1949;3:625–31.
12. Garcia S, Jardine K, Souza V, Souza R, Duvoisin Junior S, Gonçalves J. Reassimilation of Leaf Internal CO<sub>2</sub> Contributes to Isoprene Emission in the Neotropical Species *Inga edulis* Mart. *Forests.* 2019;10:472.
13. Heskell MA, Atkin OK, Turnbull MH, Griffin KL. Bringing the Kok effect to light: A review on the integration of daytime respiration and net ecosystem exchange. *Ecosphere.* 2013;4:art98.
14. Yin X, Niu Y, van der Putten PEL, Struik PC. The Kok effect revisited. *New Phytol.* 2020;227:1764–75.
15. Tcherkez G, Gauthier P, Buckley TN, Busch FA, Barbour MM, Bruhn D, et al. Leaf day respiration: low CO<sub>2</sub> flux but high significance for metabolism and carbon balance. *New Phytol.* 2017;216:986–1001.
16. Tcherkez G, Gauthier P, Buckley TN, Busch FA, Barbour MM, Bruhn D, et al. Tracking the origins of the Kok effect, 70 years after its discovery. *New Phytol.* 2017;214:506–10.
17. Sauer A, Heise KP. On the light dependence of Fatty Acid synthesis in spinach chloroplasts. *Plant Physiol.* 1983;73:11–5.
18. Gauthier PPG, Saenz N, Griffin KL, Way D, Tcherkez G. Is the Kok effect a respiratory phenomenon? Metabolic insight using <sup>13</sup>C labeling in *Helianthus annuus* leaves. *New Phytol.* 2020;228:1243–55.
19. Eprintsev AT, Fedorin DN, Dobychnina MA, Igamberdiev AU. Regulation of expression of the mitochondrial and peroxisomal forms of citrate synthase in maize during germination and in response to light. *Plant Sci.* 2018;272:157–63.
20. Plain C, Gerant D, Maillard P, Dannoura M, Dong Y, Zeller B, et al. Tracing of recently assimilated carbon in respiration at high temporal resolution in the field with a tuneable diode laser absorption spectrometer after in situ <sup>13</sup>CO<sub>2</sub> pulse labelling of 20-year-old beech trees. *Tree Physiol.* 2009;29:1433–45.
21. Meinzer FC, Brooks JR, Domec JC, Gartner BL, Warren JM, Woodruff DR, et al. Dynamics of water transport and storage in conifers studied with deuterium and heat tracing techniques. *Plant Cell Environ.* 2006;29:105–14.

22. Seeger S, Weiler M. Temporal dynamics of tree xylem water isotopes: in situ monitoring and modeling. *Biogeosciences*. 2021;18:4603–27.
23. Powers EM, Marshall JD. Pulse labeling of dissolved  $^{13}\text{C}$ -carbonate into tree xylem: developing a new method to determine the fate of recently fixed photosynthate. *Rapid Commun Mass Spectrom*. 2011;25:33–40.
24. Churchland C, Weatherall A, Briones MJ, Grayston SJ. Stable-isotope labeling and probing of recent photosynthates into respired  $\text{CO}_2$ , soil microbes and soil mesofauna using a xylem and phloem stem-injection technique on Sitka spruce (*Picea sitchensis*). *Rapid Commun Mass Spectrom*. 2012;26:2493–501.
25. Doccola JJ, Wild PM. Tree injection as an alternative method of insecticide application. *Insecticides –Basic and Other Applications*. InTech, Rijeka, Croatia. 2012; 61–78.
26. Berger C, Laurent F. Trunk injection of plant protection products to protect trees from pests and diseases. *Crop Prot*. 2019;124:104831.
27. Minnich RA, Goforth BR, Paine TD. Follow the water: extreme drought and the conifer forest pandemic of 2002–2003 along the California borderland. In: Paine TD, Lieutier F, editors. *Insects and diseases of Mediterranean forest systems*. Cham: Springer International Publishing; 2016. p. 859–90.
28. Juzwik J, Appel DN, MacDonald WL, Burks S. Challenges and successes in managing oak wilt in the United States. *Plant Dis*. 2011;95:888–900.
29. Little CE. The dying of the trees: the pandemic in America's forests. [pdfs.semanticscholar.org](https://pdfs.semanticscholar.org/); 1995.
30. Navarro C, Fernández-Escobar R, Benlloch M. A low-pressure, trunk-injection method for introducing chemical formulations into olive trees. *J Amer Soc Hort Sci*. 1992;117:357–60.
31. Guillot O, Bory G. Trunk insertion: a solution to urban trees chemical protection? *Acta Hortic*. 1999;:137–46.
32. Lehmann M. First results of neem application by tree infusion and trunk-painting against leaf destroying insects. *Proceedings of the 9th Workshop*.
33. Keil HL. Control of bacterial spot (caused by *Xanthomonas pruni*) in apricot trees by trunk infusion with oxytetracycline. *Plant Disease Reporter*. 1979.
34. Reil WO, Beutel J. A pressure machine for injecting trees. *California Agriculture*. 1976.
35. Postma J, Goossen-van de Geijn H. Twenty-four years of Dutch Trig® application to control Dutch elm disease. *Biocontrol*. 2016;61:305–12.
36. Fernández-Escobar R, Barranco D, Benlloch M. Overcoming iron chlorosis in olive and peach trees using a low-pressure trunk-injection method. *Horts*. 1993;28:192–4.
37. Dal Maso E, Cocking J, Montecchio L. An enhanced trunk injection formulation of potassium phosphite against chestnut ink disease. *Arboricultural Journal*. 2017;39:125–41.
38. Zhou XM, MacKenzie AF, Madramootoo CA, Smith DL. Effects of stem-injected plant growth regulators, with or without sucrose, on grain production, biomass and photosynthetic activity of

- Field-Grown Corn Plants. *J Agro Crop Sci.* 1999;183:103–10.
39. Petracek PD, Silverman FP, Greene DW. A history of commercial plant growth regulators in apple production. *horts.* 2003;38:937–42.
  40. Gauthier PPG, Battle MO, Griffin KL, Bender ML. Measurement of gross photosynthesis, respiration in the light, and mesophyll conductance using H<sub>2</sub><sup>18</sup>O labeling. *Plant Physiol.* 2018;177:62–74.
  41. Loreto F, Velikova V, Di Marco G. Respiration in the light measured by <sup>12</sup>CO<sub>2</sub> emission in <sup>13</sup>CO<sub>2</sub> atmosphere in maize leaves. *Functional Plant Biol.* 2001;28:1103.
  42. Farquhar GD, Busch FA. Changes in the chloroplastic CO<sub>2</sub> concentration explain much of the observed Kok effect: a model. *New Phytol.* 2017;214:570–84.
  43. Tcherkez G, Boex-Fontvieille E, Mahé A, Hodges M. Respiratory carbon fluxes in leaves. *Curr Opin Plant Biol.* 2012;15:308–14.
  44. Tcherkez G, Cornic G, Bligny R, Gout E, Ghashghaie J. In vivo respiratory metabolism of illuminated leaves. *Plant Physiol.* 2005;138:1596–606.
  45. Tcherkez G, Mahé A, Gauthier P, Mauve C, Gout E, Bligny R, et al. In folio respiratory fluxomics revealed by <sup>13</sup>C-isotopic labeling and H/D isotope effects highlight the noncyclic nature of the tricarboxylic acid “cycle” in illuminated leaves. *Plant Physiol.* 2009;151:620–30.
  46. Oliver DJ, Nikolau BJ, Wurtele ES. Acetyl-CoA—Life at the metabolic nexus. *Plant Sci.* 2009;176:597–601.
  47. Schwer B, Bunkenborg J, Verdin RO, Andersen JS, Verdin E. Reversible lysine acetylation controls the activity of the mitochondrial enzyme acetyl-CoA synthetase 2. *Proc Natl Acad Sci USA.* 2006;103:10224–9.
  48. Kunze M, Pracharoenwattana I, Smith SM, Hartig A. A central role for the peroxisomal membrane in glyoxylate cycle function. *Biochim Biophys Acta.* 2006;1763:1441–52.
  49. Beevers H. Metabolic production of sucrose from fat. *Nature.* 1961;191:433–6.
  50. Eastmond PJ, Germain V, Lange PR, Bryce JH, Smith SM, Graham IA. Postgerminative growth and lipid catabolism in oilseeds lacking the glyoxylate cycle. *Proc Natl Acad Sci USA.* 2000;97:5669–74.
  51. Füßl M, König A-C, Eirich J, Hartl M, Kleinknecht L, Bohne A-V, et al. Dynamic light- and acetate-dependent regulation of the proteome and lysine acetylome of *Chlamydomonas*. *Plant J.* 2022;109:261–77.
  52. Jardine K, Chambers J, Alves EG, Teixeira A, Garcia S, Holm J, et al. Dynamic balancing of isoprene carbon sources reflects photosynthetic and photorespiratory responses to temperature stress. *Plant Physiol.* 2014;166:2051–64.

## Figures

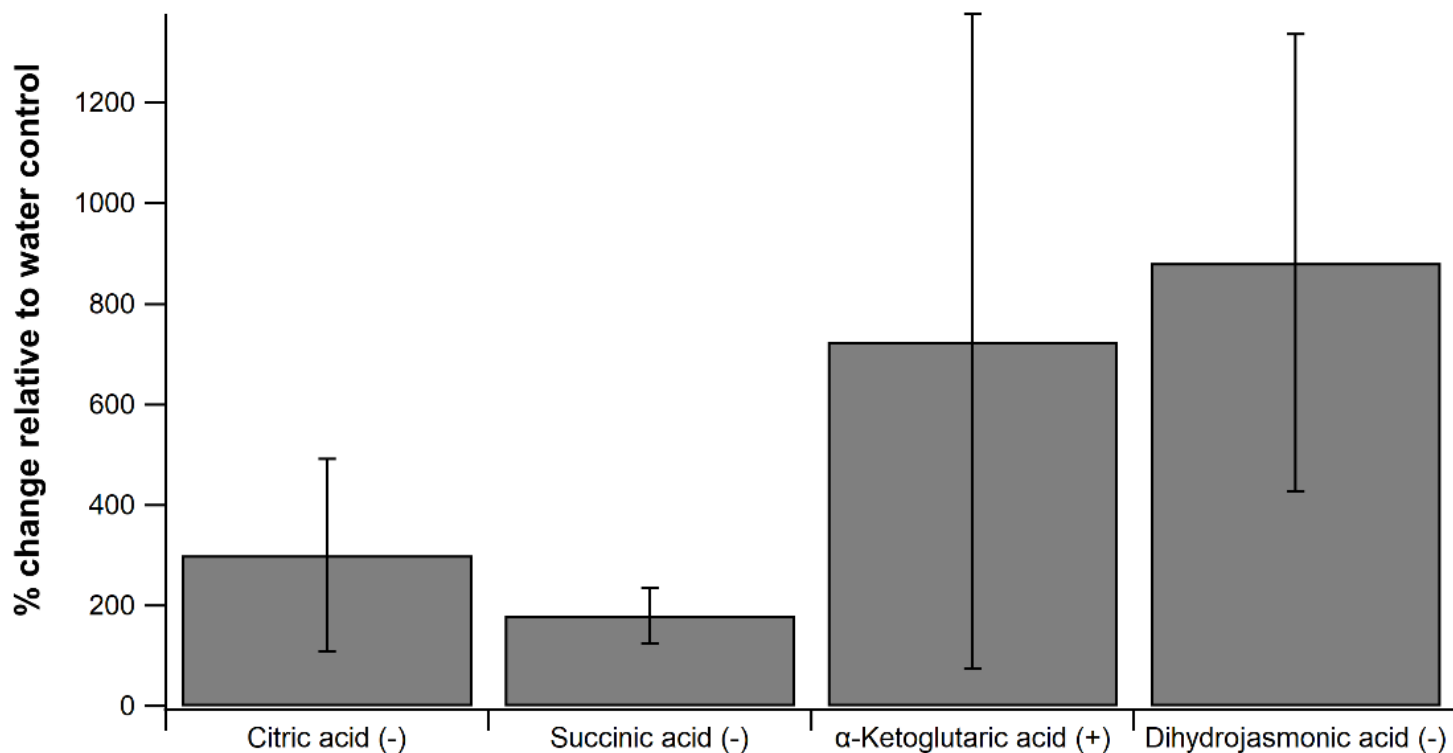


**Figure 1**

Average changes in leaf concentrations of TCA cycle intermediates Citric acid, Succinic acid, and  $\alpha$ -Ketoglutaric acid relative to water fed controls from three detached poplar branches treated with 10 mM acetate via the transpirations stream. Also shown are the relative changes in leaf concentrations of the phytohormone Dihydrojasmonic acid. Relative changes in leaf metabolite concentrations were determined by LC-MS (Liquid Chromatography Mass Spectrometry) operating in negative (-) and positive (+) modes.

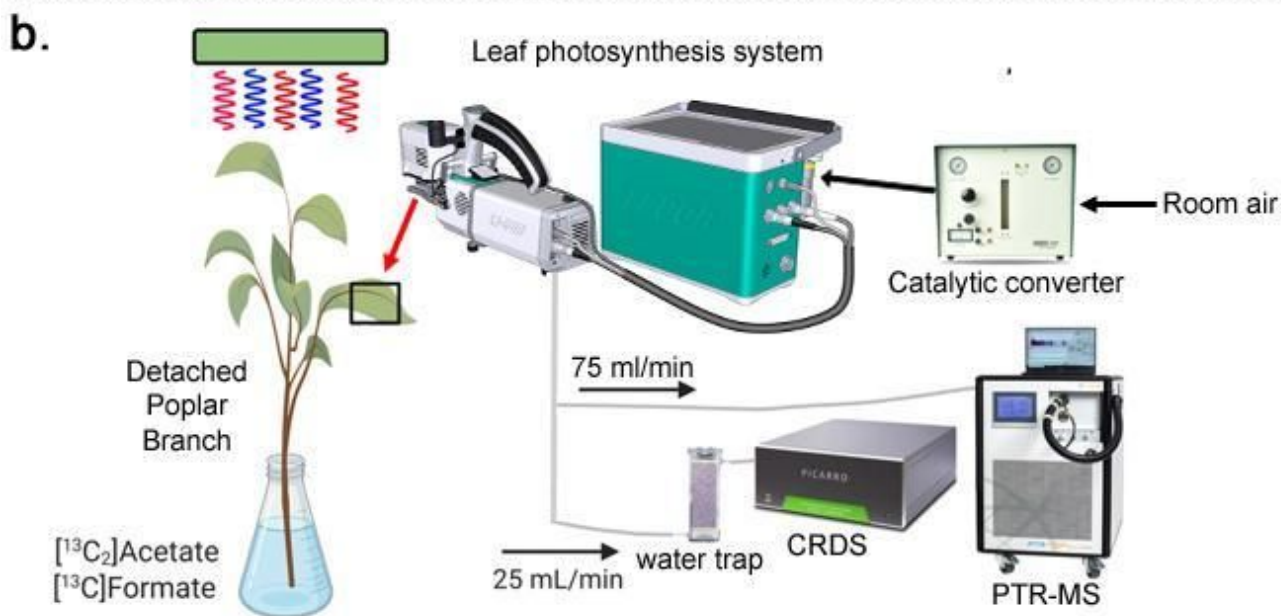
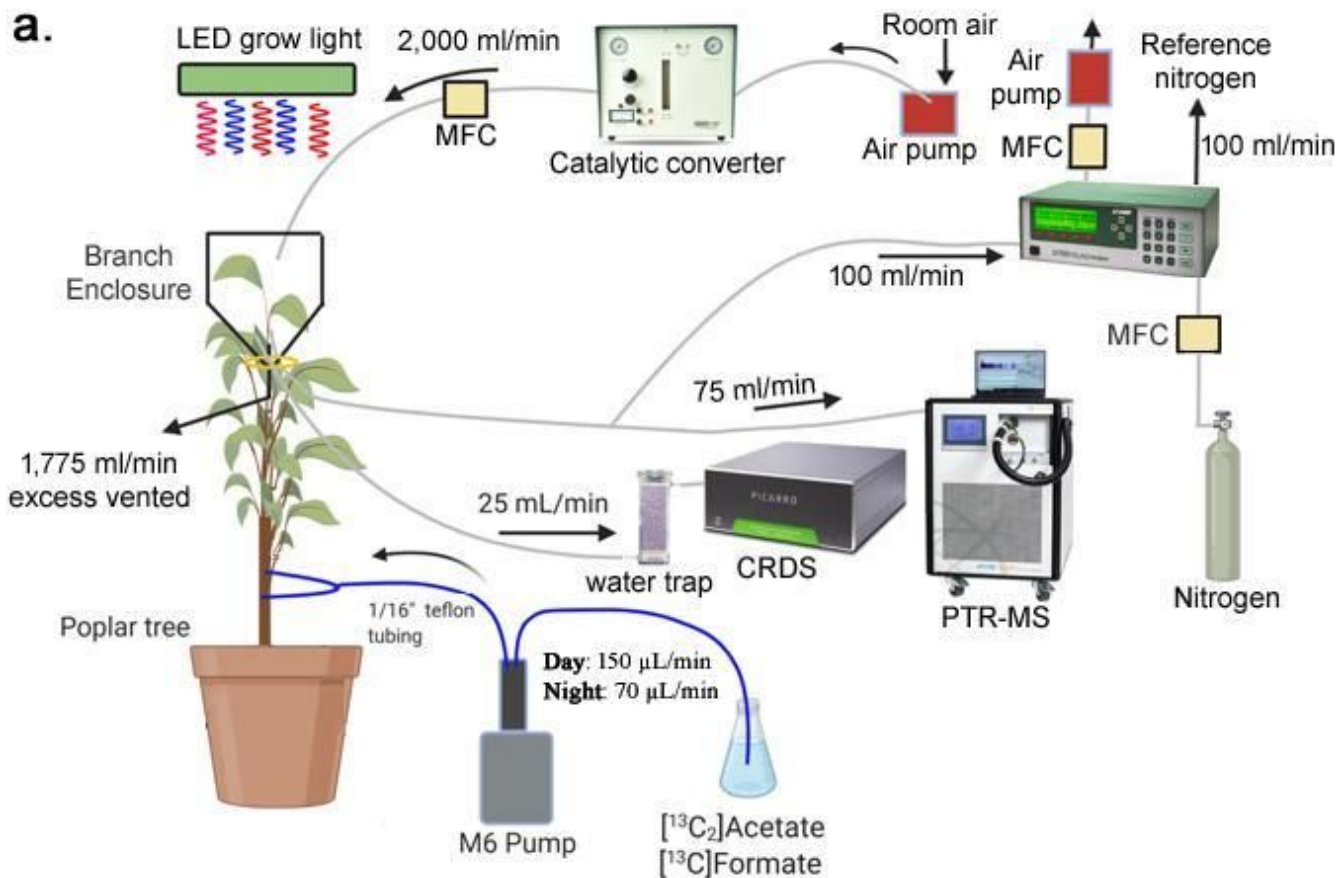


**Figure 2**

Graphical representation of whole tree/branch DXSI experiments and detached branch/leaf experiments with [ $^{13}\text{C}_2$ ]acetate and [ $^{13}\text{C}$ ]formate solutions. The DXSI experimental setup (**a**) consists of a M6 pump programmed to deliver a diurnal solution dispensing method into the xylem of 70  $\mu\text{L}/\text{min}$  (night) and 150  $\mu\text{L}/\text{min}$  (day), and real-time branch gas exchange measurements of  $\text{CO}_2$ ,  $\text{H}_2\text{O}$ , and isoprene fluxes

together with  $\delta^{13}\text{C}\text{O}_2$  analysis under constant daytime lighting. Hydrocarbon free room air was continuously delivered to a branch enclosure (2,000 ml/min) to create a dynamic flow through gas-exchange system containing one of the top branches in the upper canopy (~2 m height) with 5-10 leaves. (b) Detached branches pretreated for 1 day with a 10 mM solution of  $[\text{C}^{13}_2]\text{acetate}$  or  $[\text{C}^{13}]\text{formate}$  were studied for leaf gas exchange under controlled environmental conditions using a Li6800 system. Real-time branch and leaf isoprene emissions and  $\delta^{13}\text{C}\text{O}_2$  were quantified using PTR-MS and CRDS.  $\text{CO}_2$  and  $\text{H}_2\text{O}$  fluxes were quantified using a Li6800 (leaf) or Li7000 (branch).

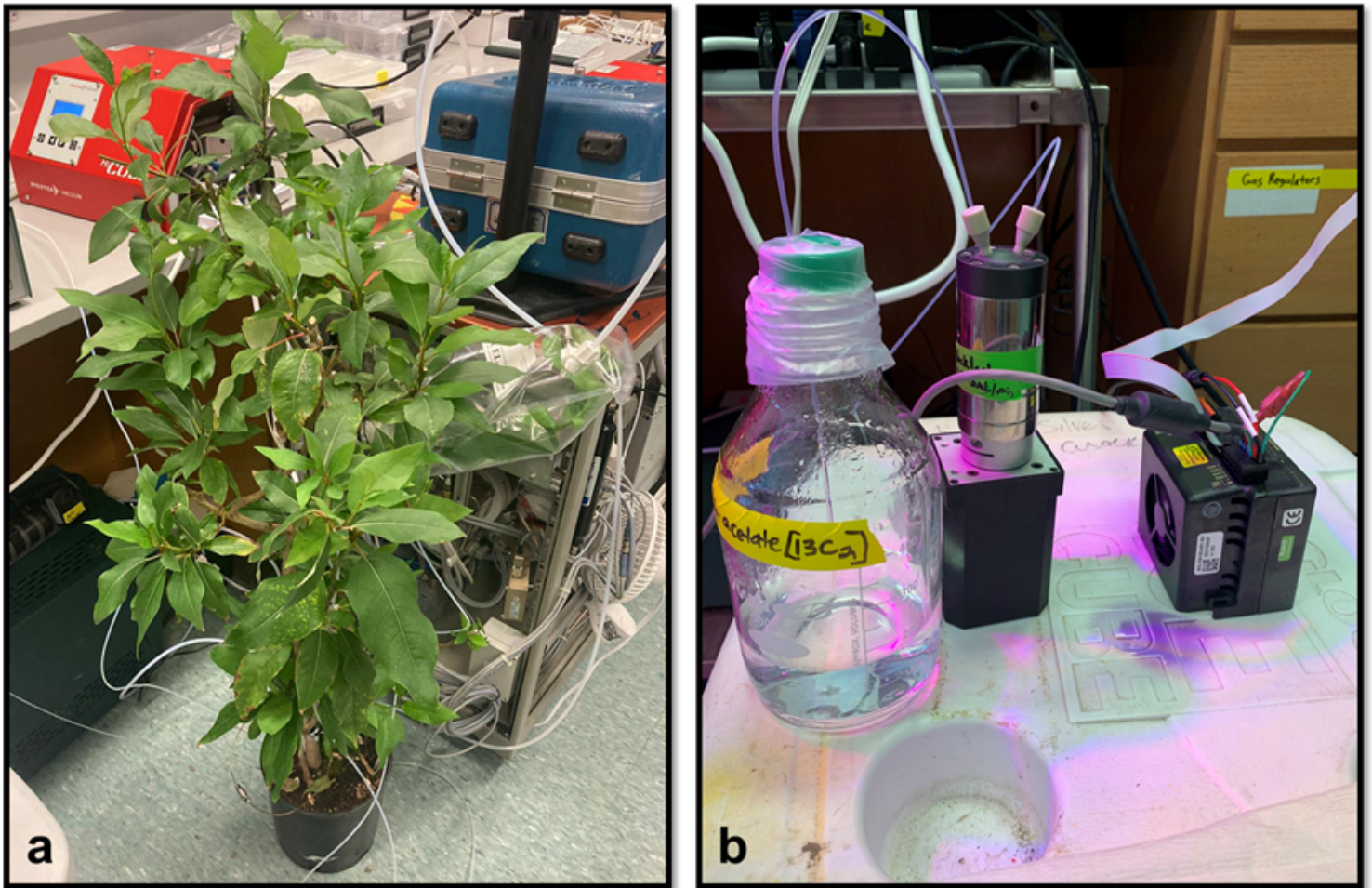


**Figure 3**

Images showing the a) DXSI experimental set-up in the laboratory and b) M6 pump and 500 mL solution reservoir.

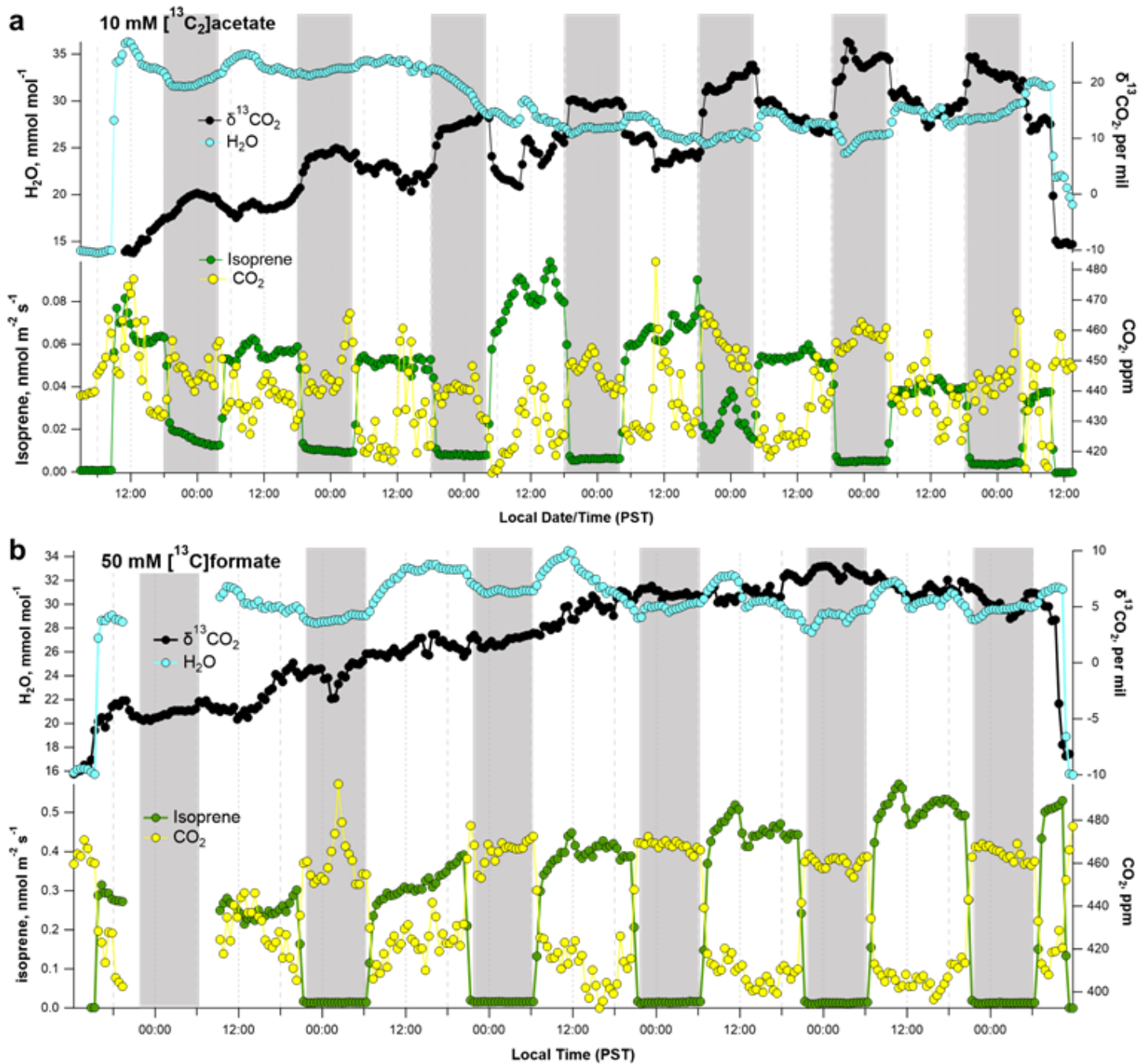


**Figure 4**

7-day time series of headspace  $\text{CO}_2$  and  $\text{H}_2\text{O}$  water vapor concentrations, isoprene emissions, and headspace with  $\delta^{13}\text{CO}_2$  in a dynamic poplar branch enclosure during a DXSI experiment using (a) a 10.0 mM solution of [<sup>13</sup>C<sub>2</sub>]acetate and (b) a 50 mM solution of [<sup>13</sup>C]formate. The first and last part of the time series is an empty branch chamber.

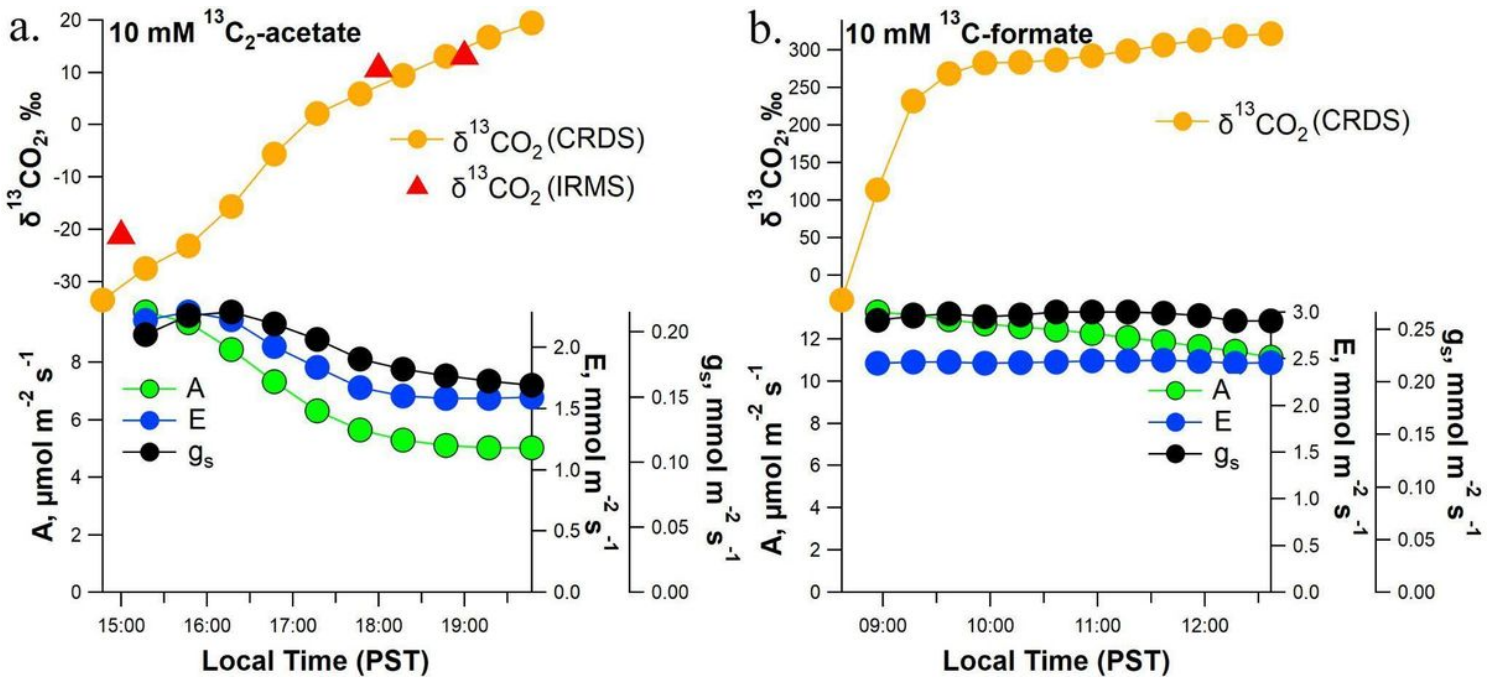
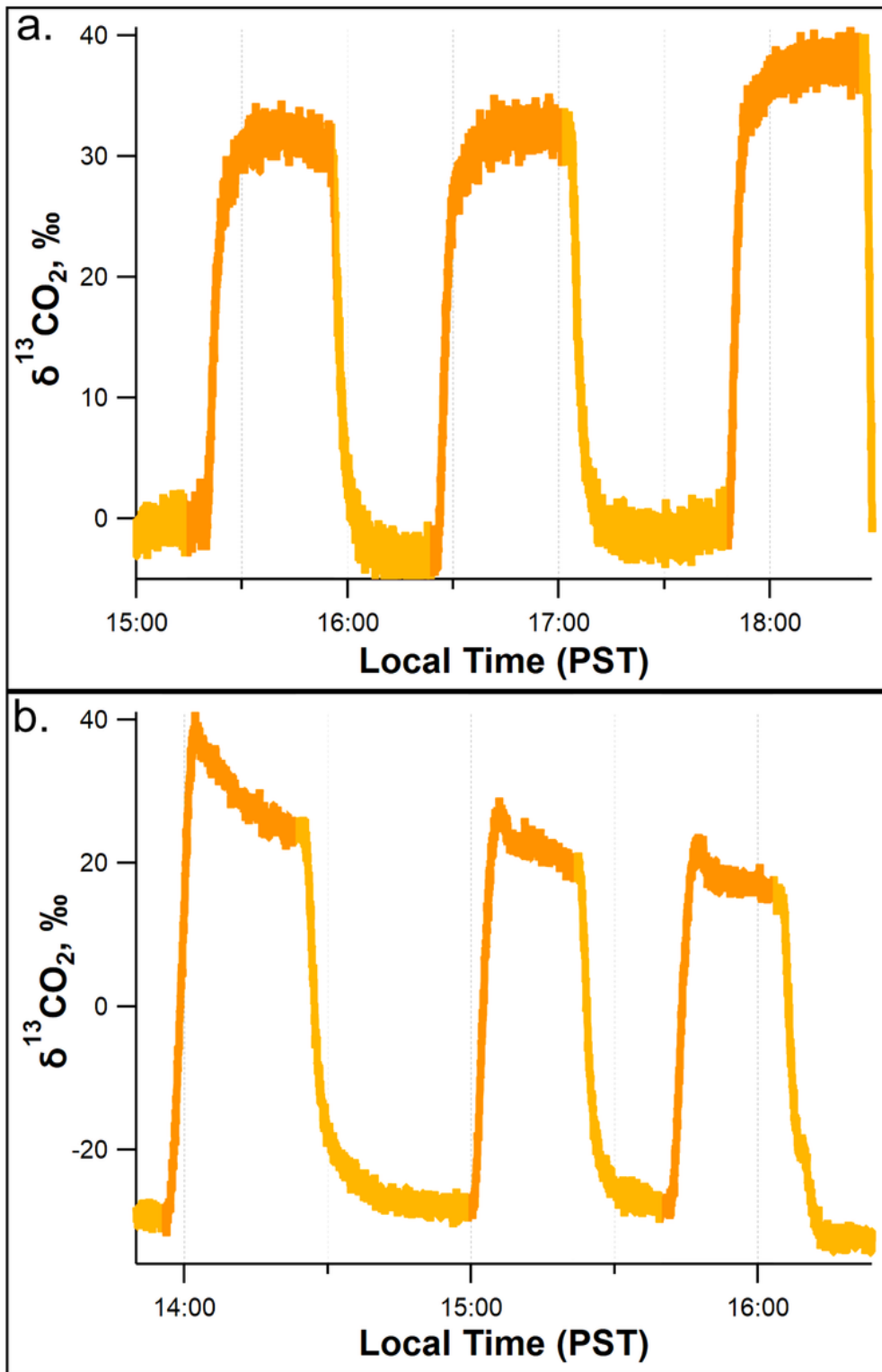


Figure 5

Example observations of leaf headspace  $\delta^{13}\text{CO}_2$  and leaf gas exchange parameters ( $A$ ,  $E$ ,  $g_s$ ) under constant environmental conditions in the light from detached poplar branches following 1-day delivery of a 10.0 mM solution of **a)** [ $^{13}\text{C}_2$ ]acetate and **b)** [ $^{13}\text{C}$ ]formate via the transpiration stream. Note the stronger  $^{13}\text{C}$ -enrichment of headspace  $\text{CO}_2$  under [ $^{13}\text{C}$ ]formate relative to [ $^{13}\text{C}_2$ ]acetate.



**Figure 6**

Rapid and reversible light inhibition of leaf headspace  $\delta^{13}\text{CO}_2$  from detached poplar branches following pretreatment with 10.0 mM [ $^{13}\text{C}_2$ ]acetate via the transpiration stream. Two example time series (a. and b.) of leaf headspace  $\delta^{13}\text{CO}_2$  during three replicate light-dark and dark-light cycles under controlled environmental conditions. Note the reversible  $^{13}\text{C}$ -enrichment of headspace  $\delta^{13}\text{CO}_2$  upon leaf darkening.

## Supplementary Files

This is a list of supplementary files associated with this preprint. Click to download.

- [SupplementaryFigs17Mar2022.docx](#)